Modeling the heat treatment of sintered $SmCo_5$ magnets

M. F. de Campos[1], J. A. de Castro[2], P. R. Rios[2]

[1]Prédio 3 - DIMAT - Instituto Nacional de Metrologia, Normalização e Qualidade Industrial-INMETRO, Rua Nossa Senhora das Graças 50 (Xerém), 25250-020 Duque de Caxias, RJ, Brasil
[2] EEIMVR-UFF, Av. dos Trabalhadores 420, 27255-125 Volta Redonda, RJ, Brasil.
Mfcampos@inmetro.gov.br

Keywords: $SmCo_5$ magnets, Heat Treatment, Finite Volume Method.

Abstract: The processing of $SmCo_5$ sintered magnets involves a post-sintering heat treatment, where the intrinsic coercivity of the magnets may increase more than one order of magnitude. Variables of the heat treatment like time, temperature and cooling rate have strong influence on coercivity. We describe a method for modeling the heat treatment, which includes microstructural features as precipitate size and 2nd phase volume fraction. The numerical solution was obtained using the Finite Volume Method to solve Fick´s second law. Experimental data like the diffusion coefficient of Sm into $SmCo_5$ phase and the Sm-Co phase Diagram are used for the modeling.

Introduction

The coercivity of $SmCo_5$ magnets made by powder metallurgy depends strongly on a post-sintering heat treatment [1]. It was proposed [2,3] that the increase of coercivity is related to the elimination of point-like defects. Previous studies [4,5] of the heat-treatment kinetics of $SmCo_5$ magnets have indicated that the kinetics of coercivity increase is compatible with the elimination of equilibrium excess-Sm atoms from the $SmCo_5$ lattice. The objective is applying the Finite Volume Method to perform a more realistic simulation of the heat treatment kinetics in $SmCo_5$, taking into account the Sm-Co Phase Diagram data [6].

Methodology

The FVM ("Finite Volume Method") with adaptative mesh in a generalized coordinate system [7,8] was used to discretise the diffusion equation representing the motion of the samarium atoms inside the $SmCo_5$ matrix. The diffusion process of samarium in the matrix was modeled [8,9] with basis on the Eq. 1 (Fick´s second law).

$$\frac{\partial(S_m)}{\partial t} = \mathrm{div}\left(D_{S_m}^{S_m Co_5} \ \mathrm{grad}(S_m) \right) \tag{1}$$

With the following boundary conditions:

$$\text{At} \quad r = R_p(t) \ \rightarrow \ S_m = S_m(t)\big|_{\text{equilibrium}} \tag{2}$$

$$\text{At} \quad r = R_m \ \rightarrow \ \frac{d(S_m)}{dr} = 0 \tag{3}$$

In the above equations (Eq. 1-3) , r – is radial position [m] ; Sm – is samarium mass fraction [kg/kg], $D_{Sm}^{S_m Co_5}$ - diffusion coefficient of the samarium atoms into the $SmCo_5$ [m^2/s], t- time [s].

The Samarium diffusion coefficient (Eq. 4) follows an Arrhenius type correlation according Kimura et al [10].

$$D_{S_m}^{S_m Co_5} = 6.90 \times 10^{-5} \exp\left(\frac{-220000}{RT}\right) \quad (4)$$

It is assumed, for initial condition, that the equilibrium is valid at the boundary of the precipitated and the matrix is supersaturated in samarium. The values summarized in Table 1 were graphically taken from the Sm-Co equilibrium diagram [6]. The calculations were carried out until the matrix concentration reached 99.99% of the equilibrium conditions for all cases simulated. The model is simulating the elimination of Sm-excess atoms (or Co-vacancies) from the matrix $SmCo_5$ lattice. The parameters representing the diffusion length were calculated based on the following equations:

$$L_p = 4\frac{V_{vp}}{S_{vp}} \quad (5a)$$

$$L_m = 4\left(\frac{1-V_{vp}}{S_{vp}}\right) \quad (5b)$$

Where $V_{vp}[m^3/m^3]$ is the volumetric fraction of the precipitate and S_{vp} $[m^2/m^3]$ is the interfacial area between the precipitated and the matrix per unit of volume. These parameters are directly calculated at the beginning of the simulation and at the end since the precipitated size increases as the diffusion process occurs. The calculation is performed by assuming for each time step a fixed mesh and the total amount of mass diffusion is computed, then a new mesh is generated in order to account for the mass balance. The re-meshing of the whole domain is accompanied by a 3D procedure of interpolation for proper considerations of the variables values in the new time step. The grid generation is made by successive refinement of the region near the interface precipitated-matrix where the concentration gradient is high. The grid used a 3D solid angle with a high refinement on the radial direction (5x80x5= 2000 finite control volumes).

Table 1 Equilibrium concentration obtained from the Sm-Co diagram [6]

Temperature (^oC)	1200	1150	1100	1050	1000	950	900	850
Sm [%]	34.6	34.3	34.2	34.1	34.0	33.9	33.85	33.8

Results and Discussion

Table 2 Predicted parameters for the heat treatments. Simulated until 99.99% of conversion.

V_v(%)	R_p(μm) initial	time(min) Isothermal	Time(min) Step-cooling	R_p(μm) – Final	Lp – Inicial (μm)	Lp – Final (μm)	Lm – Inicial (μm)	Lm- Final (μm)
1	2.5	1185	1107	2.79	3.24	3.62	329.8	262.3
2.5	2.5	536	547	2.62	3.23	3.39	129.8	116.9
5	2.5	273	331	2.56	3.24	3.32	63.32	60.12
1	5	4318	4320	5.58	6.48	7.24	659	524.9
2.5	5	2118	1968	5.24	6.48	6.79	259.8	235.6
5	5	1085	1018	5.12	6.48	6.64	127.47	120.9

R_p = precipitate radii.

In the present study, the isothermal treatment at 850 °C is compared with a step-cooling treatment comprising 30 minutes at 1050 °C – 30 minutes at 1000°C– 30 minutes at 950 °C 30 min at 900 °C and the remaining time at 850 °C. The calculation is stopped when the average samarium concentration in the matrix reached 99.99% of the equilibrium concentration at 850 °C. Table 2 summarizes technological parameters for several cases of volume fraction of 2nd phase and size of precipitates. It was assumed in the simulation that the 2nd phase precipitate is Sm_2Co_7, but it also could be Sm_5Co_{19} [2]. The same calculations were performed supposing completion done for 90% of conversion, and these results are shown in Table 3. The magnitude order of Lambda - Lm - (10^2 μm) is compatible with the estimate from a previous model [4,5], see Tables 2 and 3.

Table 3 Predicted parameters for the heat treatments. Simulated until 90 % of conversion.

V_v(%)	R_p(μm) initial	time(min) Isothermal	Time(min) Step-cooling	R_p(μm) - Final	Lp – Inicial (μm)	Lp – Final (μm)	Lm – Inicial (μm)	Lm- Final (μm)
1	2.5	308	228	2.76	3.24		329.8	
2.5	2.5	137	148	2.61	3.24	3.38	129.8	118.7
5	2.5	69	129	2.55	3.24	3.30	63.32	60.6
1	5	1224	919	5.52	6.48	7.15	659	538
2.5	5	542	377	5.22	6.48	6.77	259.8	237
5	5	271	207	5.11	6.48	6.62	127.47	120.7

Isothermal heat treatment

In the calculation for the isothermal treatment at 850 °C, we have assumed that the heat treatment is completed when the averaged samarium concentration of the matrix reached 99.99% of the equilibrium value at this temperature. As stated above, these values were taken from the Sm-Co equilibrium diagram [6]. Results obtained for several different conditions are shown in Figs. 1-4.

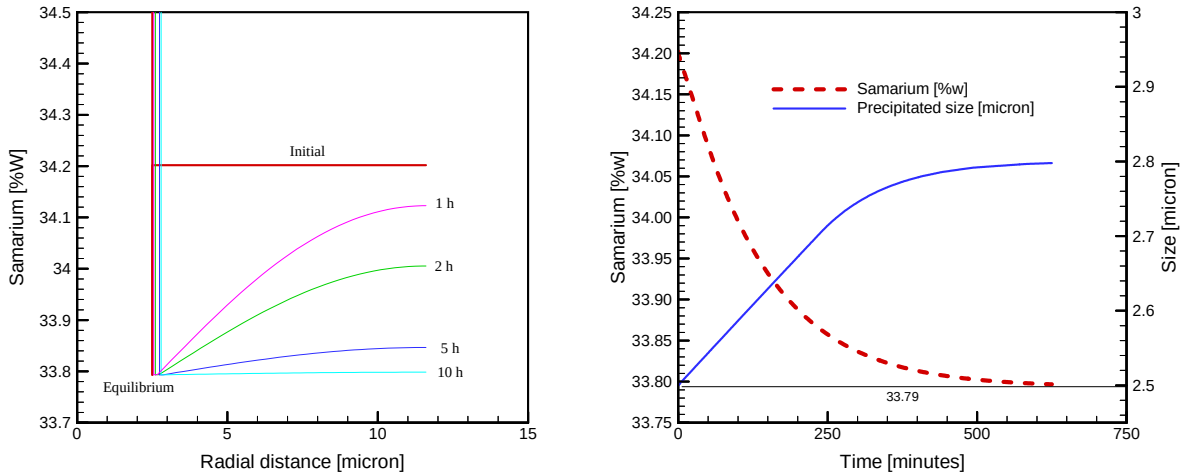

(a) (b)

Figure 1. (a) Samarium distribution in the radial distance within the matrix (1% volume and Rp(initial)=2.5 micron. (b) time evolution of samarium averaged concentration within the matrix and precipitated size (1% volume and Rp(initial)=2.5 micron).

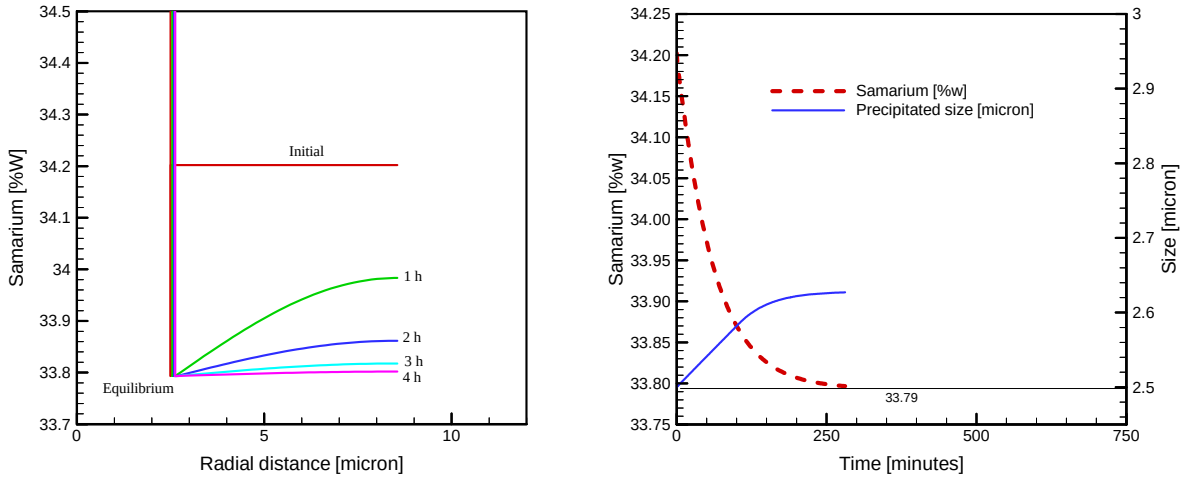

(a) (b)

Figure 2. (a) Samarium distribution in the radial distance within the matrix (2.5% volume and Rp(initial)=2.5 micron. (b) time evolution of samarium averaged concentration within the matrix and precipitated size (2.5% volume and Rp(initial)=2.5 micron).

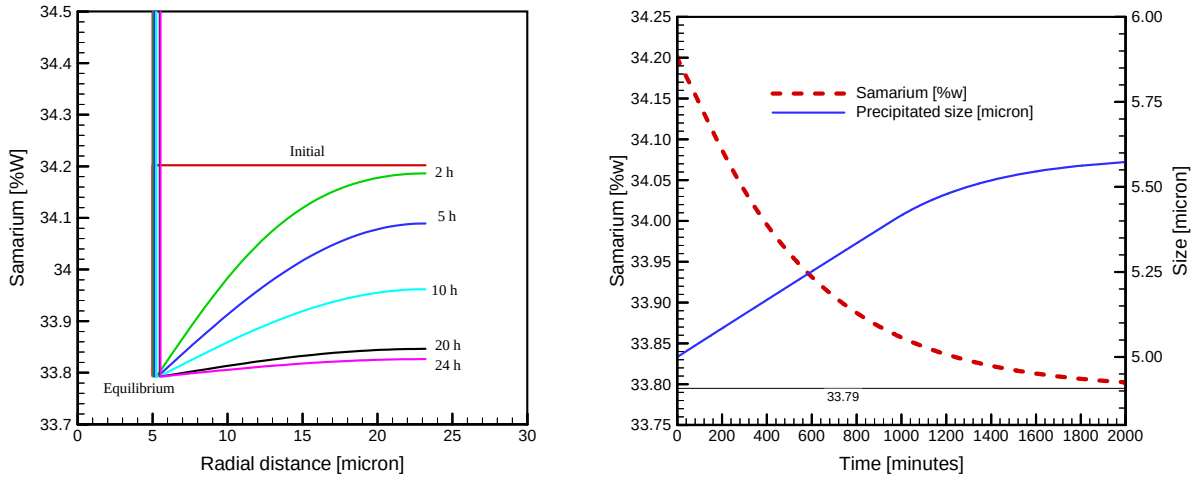

(a) (b)

Figure 3. (a) Samarium distribution in the radial distance within the matrix (1% volume and Rp(initial)=5 micron. (b) time evolution of samarium averaged concentration within the matrix and precipitated size (1% volume and Rp(initial)=5 micron).

The comparison between Figs. 1-4 shows that the elimination of Sm-excess from $SmCo_5$ matrix phase strongly depends on the radius (R_p) and volume fraction of the 2nd phase precipitate.

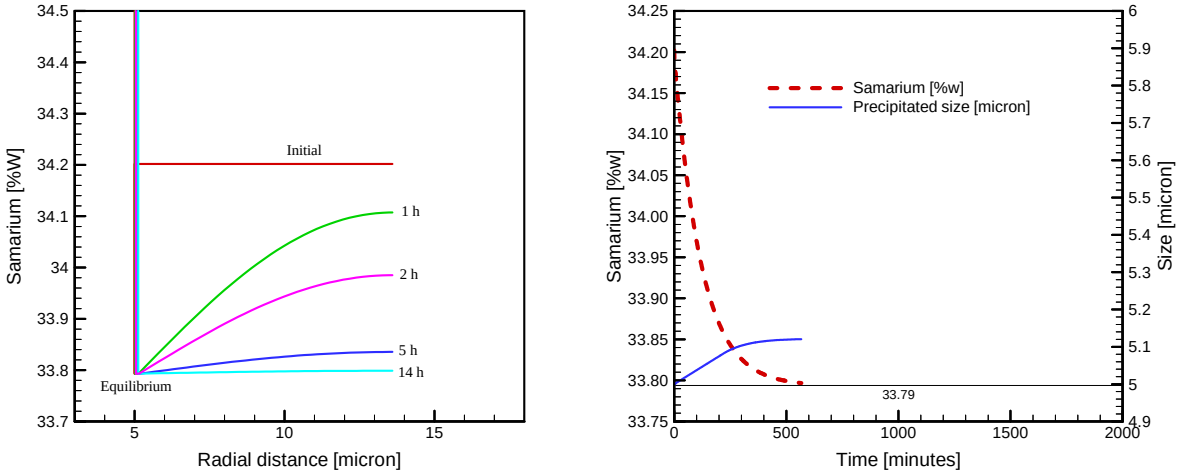

(a) (b)

Figure 4. (a) Samarium distribution in the radial distance within the matrix (5% volume and Rp(initial)=5 micron. (b) time evolution of samarium averaged concentration within the matrix and precipitated size (5% volume and Rp(initial)=5 micron).

Step-cooling heat treatment

In this section, a step-cooling heat treatment, from 1100°C to 850°C remaining ½ hour at each step (1050, 1000, 950 and 900°C) will be compared with an isothermal heat treatment at 850°C. The objective is achieving a better understanding of the result reported by Martin et al [1]. The results of the simulation (Figs. 5 and 6) indicate that non-isothermal is more favorable when 2nd phase volume fraction is small (or also when the radius of the precipitated of 2nd phase is larger). Since the industrial practice is minimizing 2nd phase volume fraction (to maximize the remanence of the magnets), this is compatible with the heat treatment typically employed by industry. However, when the volume fraction is high enough (5%, as showed in Fig. 6b), the step cooling is advantageous. Thus, we may suppose that the samples used by Martin et al [1] presented 2nd phase low fraction (and possibly large precipitate size).

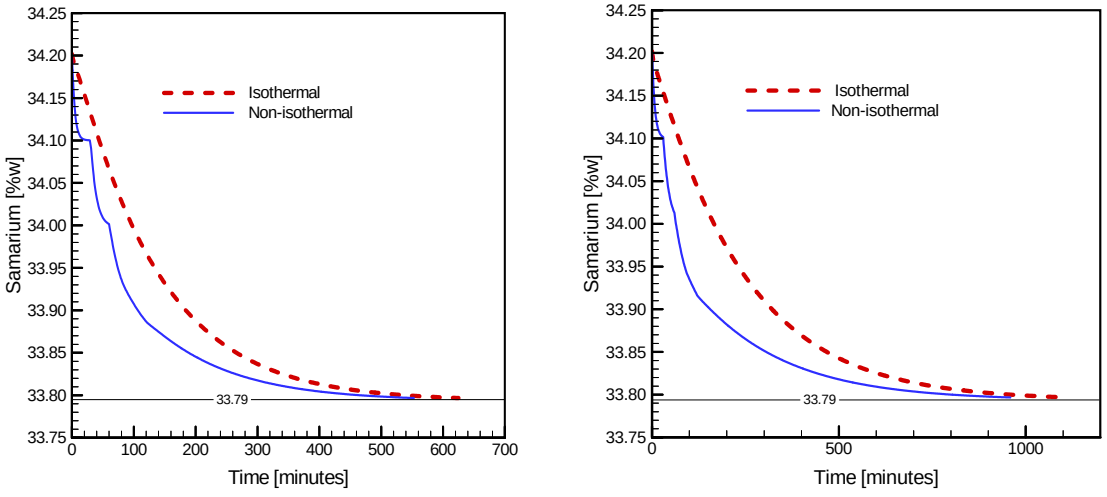

(a) (b)

Figure 5. (a) Comparison of isothermal and non-isothermal treatment (Vv=1% and Rp=2.5 micron) (b) Comparison of isothermal and non-isothermal treatment (Vv=2.5% and Rp=5 micron).

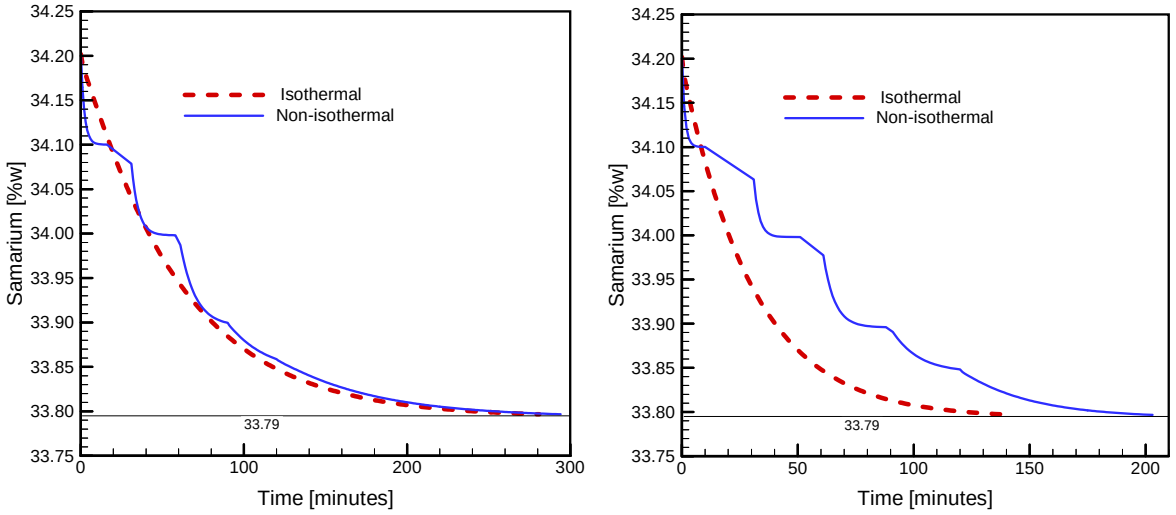

(a) (b)

Figure 6. (a) Comparison of isothermal and non-isothermal treatment (Vv=2.5% and Rp=2.5 micron) (b) Comparison of isothermal and non-isothermal treatment (Vv=5% and Rp=2.5 micron).

Conclusions

The simulation allowed the estimation of the heat treatment completion times for different microstructures. The times that were found are compatible with those employed by industry. The magnitude order of Lambda Lm (10^2 μm) is compatible with the estimate from a previous model [4,5] for a commercial heat treatment. The results indicate that elimination of Sm-excess from $SmCo_5$ matrix phase strongly depends on the radii and volume fraction of the 2nd phase precipitate.

Acknowledgements

This work was supported by Conselho Nacional de Desenvolvimento Científico e Tecnológico, CNPq, Coordenação de Aperfeiçoamento de Pessoal de Nível Superior, CAPES, and Fundação de Amparo à Pesquisa do Estado do Rio de Janeiro, FAPERJ.

References

[1] D. L. Martin, R. P. LaForce, M. G. Benz, Gen. Electr. Techn. Rep. 73 CRD 140 (1973).
[2] M. F. de Campos, F. J. G. Landgraf. In: Proc. of 16th International Workshop on Rare-Earth Magnets and their Applications. (Sendai, Japan, 2000), p. 297-306.
[3] M. F. de Campos, H. Okumura, G. C. Hadjipanayis, D. Rodrigues, F.J.G. Landgraf, A.C. Neiva, S. A. Romero, F.P. Missell, J. Alloys. Compd. 368 (2004), p. 304-307.
[4] M. F. de Campos, P. R. Rios, J. Alloys. Compd. 377 (2004), p. 121-126.
[5] M. F. de Campos, P. R. Rios. In: Proc. of 18th International Workshop on High Performance Magnets and their Applications. (Annecy, France, 2004), p. 302-309.
[6] M.F. de Campos, F.J.G. Landgraf. J. Phase Equilibria 21 (2000), p. 443-446.
[7] M.C. Melaaen, Numerical Heat Transfer B, 21 (1992), p. 1-19.
[8] J. A. Castro, H. Nogami, J. Yagi, ISIJ Int. 42 (2002), p. 44-52
[9] J. C. Slattery, *Advanced Transport Phenomena* (Cambridge University Press, 1999), p. 585-595.
[10] N. Kimura, S. Iwasaki, Y. Nakamura, J. Japan Inst. Metals, 54(1) (1990), p 48-53.